Sustainable Pavement Overlays Using Engineered Cementitious Composites

Michael D. Lepech[1+] and Victor C. Li[2]

Abstract: Contributing nearly 5% of global anthropogenic greenhouse emissions through cement production alone, the concrete industry is a major contributor to global climate change. Automobiles and trucks that use concrete transportation infrastructure release another 30% of anthropogenic greenhouse emissions. Along with these atmospheric emissions, the construction, repair, and rehabilitation of concrete pavements rely on the production and flow of large quantities of concrete material and its constituents. To reduce environmental impact and improve the sustainability of pavement overlay systems, a class of materials called Engineered Cementitious Composites (ECC) is introduced to construct more sustainable, durable rigid pavement overlays. ECC overlays are designed to enhance sustainability in two ways. First, "greener" ECC materials incorporate high volumes of industrial waste to reduce the environmental impacts of material production. Fundamental micromechanics carefully guide this green material design to maintain pseudo-strain hardening material behavior under tension. This ductile behavior, over 500 times greater than conventional concrete, is critical to the second mechanism for sustainability enhancement. The ductility of ECC suppresses reflective cracking, a major cause of premature overlay failure, thereby increasing durability and reducing life-cycle maintenance. By incorporating industrial waste, over 70% of ECC virgin constituents have been replaced without reducing critical mechanical performance characteristics. When coupled with a possible 50% reduction in overlay thickness and extension of service life as compared to conventional concrete overlays, significant sustainability improvements have been modeled. These improvements are quantitatively measured using life cycle cost and life cycle assessment techniques.

Key words: ECC; Engineered cementitious composites; Green concrete; Overlay; Sustainable pavement.

Introduction

Worldwide, roadway transportation systems are some of the most widely used, maintained, and visible public facilities. In 2006 alone, American drivers drove 3.0 trillion vehicle-miles along nearly 4 million miles of public roadways [1]. While there is little argument over the need to expand and maintain roadway infrastructure systems around the world to spur both economic development (in developing countries) and continued prosperity (in developed countries), the continuing trends of unsustainable material production, roadway construction, operation, deterioration, repeated repairs, and demolition are alarming.

Unsustainable material production for concrete pavements begins with the production of Portland cement. The mining, calcining, and grinding of Portland cement contributes nearly 5% of global anthropogenic greenhouse emissions [2], making the cement and concrete industries a major contributor to global climate change. Following this initial construction, poor maintenance of concrete pavements can lead to excessive deterioration and associated repair needs. As recently as 2009, the American Society of Civil Engineers

assigned grades of C and D to America's bridges and roads, respectively [3]. This deteriorated state can lead to repeating cycles of short-term repair scenarios, which result in increased material consumption of repair materials and fuels.

In addition to material consumption, the sustainability of pavement systems also extends to the vehicles traveling over the pavement. Automobiles and trucks release 34% of US anthropogenic greenhouse emissions [1]. Associated with every construction and maintenance event is traffic congestion that results in increased fuel use and emissions. Moreover, emissions from traffic increase as pavement roughness increases throughout service life. Together these phenomena comprise a significant piece of the unsustainable state of current concrete pavement technologies.

While increased maintenance and rehabilitation funding initiatives such as the American Recovery and Reinvestment Act in the United States are important to maintaining the infrastructure system in useable condition, greater maintenance funding will not solve the significant sustainability challenges facing concrete pavement systems. A more fundamental solution for concrete pavements, both reinforced and unreinforced, is needed that approaches both the material and system impacts described earlier. While concrete materials are both economical and simple to construct, their lack of durability has consistently been problematic. Many methods have been proposed to improve concrete durability, such as the use of high strength concrete, expensive concrete admixtures, or epoxy coated reinforcement. However, few solutions have targeted the inherent shortfall of concrete as a brittle material, which cracks under load. These cracks are the cause of most corrosion and durability problems, ultimately leading to oxidation of steel reinforcement, concrete faulting, and pavement failure. To

[1] Assistant Professor, Department of Civil and Environmental Engineering, Stanford University, Stanford, California 94305-4020, USA.
[2] E. B. Wylie Collegiate Chair, Professor, Advanced Civil Engineering Materials Research Laboratory, Department of Civil and Environmental Engineering, University of Michigan, Ann Arbor, Michigan 48109-2125, USA.
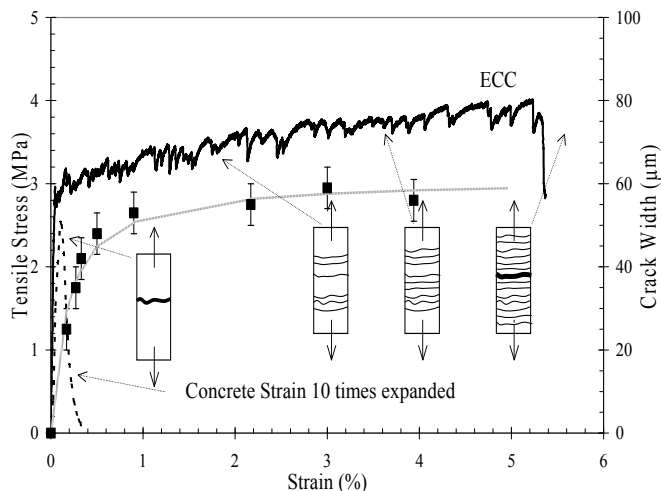[+] Corresponding Author: E-mail mlepech@stanford.edu

Fig. 1. Representative Uniaxial Tensile Stress-Strain Curve and Crack Width Development for ECC Material. For Comparison, the Tensile Behavior of Concrete is also Shown [5].

Fig. 2. Comparison between Quasi-brittle, Tension-softening, and Strain-hardening Cement-based Material Performance in Uniaxial Tension [6].

effectively solve the serious sustainability challenges facing concrete pavement, a fundamental solution reducing the brittle nature of concrete is proposed.

Engineered Cementitious Composites

A new class of cementitious materials, called Engineered Cementitious Composites (ECC) is presented in this article as an alternative to conventional rigid pavement repairs and overlays to improve the overall sustainability of these systems. Considered a type of high performance fiber reinforced cementitious composite (HPFRCC), ECC exhibits ductility similar to metals, along with inherently tight crack widths that result in highly durable ECC applications [4]. Due to this combination of large ductility and associated durability, ECC represents a new approach to the design of more sustainable pavement systems.

The most distinctive characteristic separating ECC from other concrete or cement-based materials is an ultimate strain capacity between 3 and 5%, depending on the specific ECC mixture. This strain capacity is realized through the formation of many closely spaced microcracks, allowing for a strain capacity over 300 times that of normal plain concrete. These cracks, which carry increasing load after formation, allow the material to exhibit strain hardening, similar to many ductile metals, as seen in a typical uniaxial tensile stress-strain curve (Fig. 1 [5]). While the mechanism underlying this inelastic strain is not dislocation slip on crystallographic planes, as in metals, when viewed over a representative gauge length, the deformation resulting from distributed microcracks under increasing tensile load may be interpreted as strain. This is uniquely different from typical concretes or fiber reinforced concretes (FRC) that form a single localized fracture when loaded. In the case of plain normal concrete, the crack opens wide with a rapid drop in load capacity. In the case of FRCs, the crack opens with a gradual drop in load, exhibiting a tension softening behavior. While the mechanism behind concrete and FRC deformation is similar to ECC in that it cracks, all deformation is localized at a single section (i.e. the crack face) and the concept of gauge length, and consequently strain,
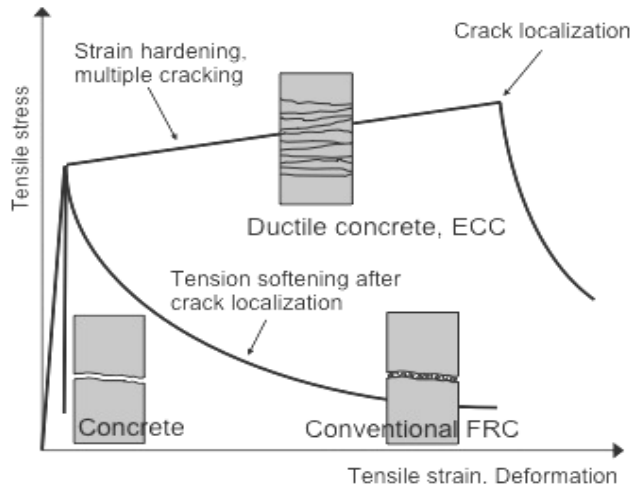
ceases to exist. The comparison between these quasi-brittle, tension-softening, and strain-hardening cement-based materials is shown in Fig. 2 [6].

Of equal importance to the strain capacity of ECC is the process by which cracks develop throughout the straining process. This is also shown in Fig. 1. After first cracking, early cracks widen with increasing load to allow for deformation. However, once a strain of approximately 1% is attained, crack widths become steady at roughly 60*mm*. Past this point, further straining is accommodated through the formation of additional microcracks until the material is saturated with microcracks at between 3 and 5% uniaxial tensile strain. At failure, a single crack ultimately localizes and the slowly drops with increased deformation, similar to a common tension softening FRC.

Unlike crack width in reinforced concrete, which is governed by steel reinforcement ratio, crack width in ECC is an inherent material property unrelated to steel reinforcing bars, if in fact these bars are present. This decoupling of crack width control from steel reinforcement ratio is another characteristic unique to ECC, allowing for expanded opportunities in jointed reinforced concrete pavement (JRCP) systems. By eliminating the dependence of crack control upon reinforcement, reinforcing steel can commonly be eliminated. Furthermore, the inherent steady-state crack width of 60*mm* significantly benefits durability considerations, exhibiting a water permeability of approximately $1.0 \times 10^{-10} m/s$ (Fig. 3 [7]), close to that of uncracked concrete. Cracking this small has also been shown to undergo limited self-healing [7, 8].

The composition of ECC is similar to many other FRCs, such that it is a mixture of cement, sand, water, fibers, and a small amount of commercial admixtures. Coarse aggregates are not used due to their adverse effect on performance. While most HPFRCCs rely on a high fiber volume to achieve high performance, ECC uses low amounts, typically 2% by volume, of short, discontinuous fiber. This low fiber volume, along with the common components, allows for mixing in conventional ready mixed concrete trucks [9]. Many HPFRCCs with fiber fractions exceeding 5% cannot conform to these conventional mixing practices.
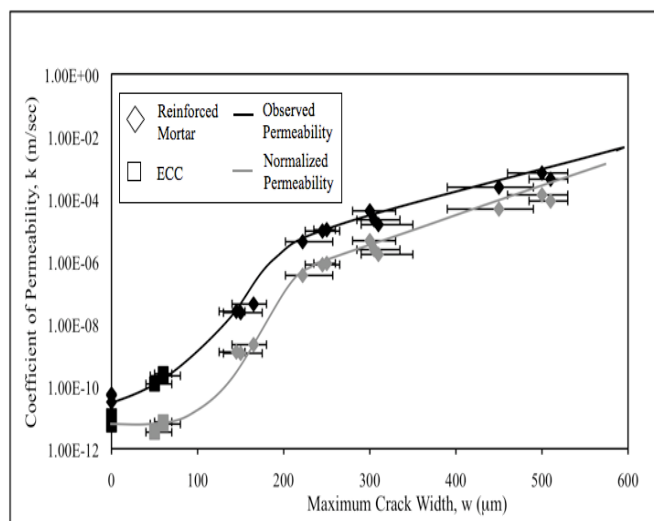
Fig. 3. Coefficient of Permeability Versus Maximum Crack Width for ECC and Reinforced Mortar Series Deformed to 1.5% Uniaxial Tension [7].

While the components of ECC may be similar to FRC, the distinctive ECC characteristic of strain hardening through microcracking is achieved through micromechanical tailoring of the components (i.e. cement, sand, and fibers), along with controlled interfacial properties between these components. Fracture properties of the cementitious matrix are controlled through cement type, sand gradation, and various admixtures. Fiber properties, such as strength, modulus of elasticity, and aspect ratio have been customized for use in ECC. The interfacial properties between fiber and matrix have also been optimized in cooperation with the manufacturer for use in this material.

ECC Mechanical and Environmental Performance in Pavement Applications

To evaluate the performance of ECC under typical transportation-related mechanical and environmental loads, durability tests and long-term performance studies on ECC materials have been conducted by the authors and other researchers. These tests include restrained shrinkage tests, fatigue and bonding tests, freeze thaw exposure, wearing/abrasion tests, and accelerated environmental tests. Additionally, the long-term strain capacity and early age strength development of ECC have been investigated. These studies confirm that ECC will successfully perform as a rigid pavement overlay material for highway applications.

Restrained Shrinkage

To examine the restrained shrinkage behavior of ECC, ring tests (AASHTO PP-34) were carried out for both ECC and normal Portland cement concrete. Due to the high cement content of ECC, significantly higher free shrinkage deformation is exhibited, compared to normal concrete [5]. However, restrained shrinkage tests show that although hygral deformation may be higher, crack widths in ECC remain below 50*mm* (50% relative humidity, RH, for 100 days), compared to concrete crack widths of approximately
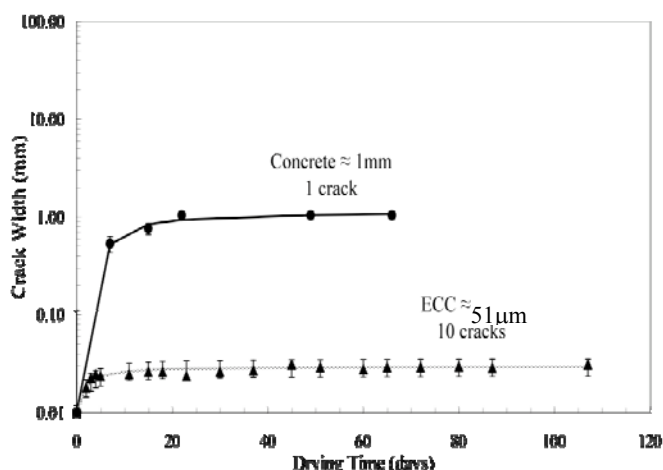

Fig. 4. Crack Width Development as a Function of Drying Time (RH=50%) [5].

1*mm* (Fig. 4). This is achieved through the microcracking of ECC, allowing the shrinkage deformation to be distributed over a large number of small cracks, while all shrinkage deformation in concrete localizes at a single crack. Further, the formation of shrinkage cracks at ECC/concrete interfaces is prevented by lower interfacial stresses due to the large deformability of ECC.

Fatigue Testing and Overlay Bond Characteristics

The fatigue characteristics of ECC were investigated to assess the performance in high fatigue scenarios, such as pavement overlays. Both ECC/concrete and concrete/concrete overlay specimens were tested in flexural fatigue [10]. In overlay applications, reflective crack propagation through the overlay is a common mode of failure. This reflective cracking reduces load capacity and result in flexural fatigue. Tests show the flexural capacity of ECC overlaid on a concrete substrate was double that of specimens with concrete overlaid on a concrete substrate. The deformability of ECC/concrete specimens was also increased while fatigue life was extended by several orders of magnitude over concrete/concrete specimens. Further, the microcracking deformation mechanism of ECC eliminates reflective crack localization.

In addition to fatigue performance and crack resistance, the bond characteristics of ECC/concrete interfaces have been investigated. Using ECC as an overlay material, the delamination and accompanying deterioration processes, typically seen in many concrete/concrete applications were not seen. Through a unique kinking-and-trapping crack formation process, both the load capacity and energy absorption of the ECC/concrete overlay was increased over concrete/concrete systems. In this mechanism, cracks propagate slightly along the bonding interface but are then directed into the ECC overlay and immediately arrested by the high ECC toughness ($34kJ/m^2$ [11]). This kinking-and-trapping process is repeated until the ECC ultimately fails in flexure, unrelated to interfacial debonding. Additionally, tests have been performed to investigate the influence of surface preparation on bonding. These tests show that regardless of a smooth or roughened interface, the bond performance of an ECC/concrete overlay is superior to that of a concrete/concrete overlay [12].
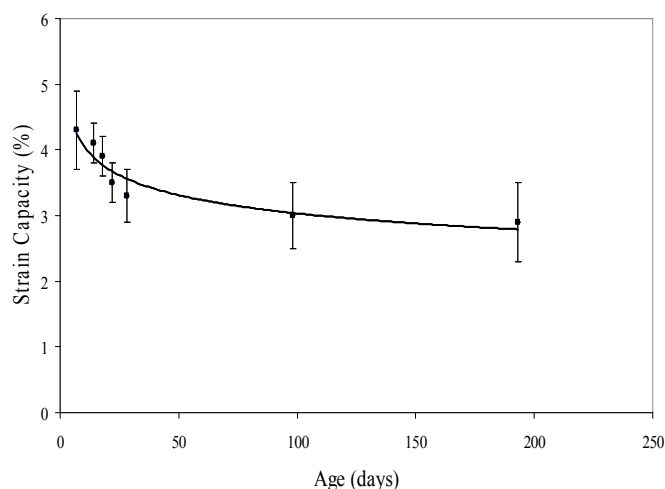
Fig. 5. Tensile Strain Capacity Development of ECC Material [15].

Freeze Thaw

Freeze thaw testing in accordance with ASTM C666A have been performed on companion series of Poly-vinyl-alcohol (PVA) fiber reinforced ECC and normal plain concrete specimens were exposed to frost cycles. In addition to dynamic modulus testing of prism specimens as outlined in C666A, a series of ECC tensile specimens were also subjected to frost cycles. This testing series evaluated the effect of frost conditions on composite strain capacity. Results from these tensile specimens were compared to tensile coupons of identical age cured in water at 22ºC.

Testing of prism specimens was conducted over 14 weeks. The ECC specimens survived the entire test duration of 300 cycles with no degradation of dynamic modulus. This performance results in a durability factor of 100 for ECC specimens, as computed according to ASTM C666. In uniaxial tension tests performed on wet cured and frost exposed ECC tensile coupons of the same age, no significant drop in strain capacity was experienced after 300 frost cycles. Both wet cured and freeze thaw specimens exhibited a strain capacity of roughly 3%, which, while lower than the 5% strain capacity mentioned above, fits closely with long term results in specimens of this age which will be discussed below. Recent work on freeze-thaw cycles in the presence of salt concentration reveals strong salt-scaling resistance and durability in ECC [13].

Abrasion and Wear Testing

For roadway surfaces, ECC must provide an adequate surface for driving and braking, while withstanding traffic abrasion. Surface friction and wear track testing was conducted in conjunction with the Michigan Department of Transportation (MDOT) to evaluate the ability of ECC to withstand wheel abrasion and provide sufficient braking friction. A set of four ECC roadway surfaces were cast corresponding to various types of surface texturing. One specimen was tined with a tining rake to produce transverse grooves; another was cured under a textured cloth to simulate wet curing under burlap; a third was textured with Astroturf to roughen the surface, a practice common in Michigan; and a final specimen was topped with coarse sand surface. Due to the presence of fibers, tining to

produce grooves or dragging items across the surface proved to be difficult, and resulted in removal of the top layer of fresh material, effectively ruining the finished surface. However, with a number of trials, adequate texturing was achieved.

Specimens were cured for 28 days and subjected to both static friction testing and wear track testing according to Michigan Test Method 111 [14]. Initial friction forces between vehicle tires operating at 65*kph* and the textured ECC specimens were determined using a static friction tester. All static friction tests were conducted on a wet pavement surfaces. Following initial friction testing, ECC specimens were subjected to 4 million tire passes to simulate long-term pavement wear. After wearing, friction forces were once again determined to assess any deterioration or surface polishing. These final friction forces are defined as the Aggregate Wear Index (AWI). AWI values for the textured ECC samples tested range from 1.6 to 2.3*kN*. The established minimum AWI for Michigan trunk line road surfaces is 1.2*kN*, lower than all ECC surfaces tested, making it a suitable material for roadway surfaces. From this testing, a transverse tined surface treatment, exhibiting an AWI of 2.3*kN* after 4 million tire passes, is currently recommended for ECC pavement surfaces. Other commonly used concrete pavement texturing methods should also be evaluated in future research to determine improved performance.

Long Term Strain Capacity

To validate the long-term viability of ECC pavements, a series of tensile tests have been performed to determine long-term strain capacity. Due to the delicate balance of cement matrix, fiber, and matrix/fiber interface properties which must be maintained to achieve strain hardening, the strain capacity of ECC material changes during the maturing process. This is exhibited in a plot of ECC strain capacity versus age (Fig. 5 [15]). Initially, strain capacity is very low due to the low strength of the matrix. For the ECC mix design shown, at roughly 10 days aging peak strain capacity is achieved due to an optimal balance of matrix, fiber, and matrix/fiber interface properties. As hydration continues, a slight imbalance occurs and remains throughout the life of the material resulting in a long-term strain capacity of 3% for ECC material. As mentioned before, this long term strain capacity data fits well with the strain capacity exhibited by freeze thaw and wet cured tensile specimens at 14 weeks. While long-term tests have only been carried out to 180 days, the long-term strain capacity has asymptotically reached approximately 3%.

Accelerated Weathering Tests

In contrast to freeze thaw tests that are designed to simulate temperature changes in harsh winter conditions, hot water immersion tests have been conducted to simulate the long term effects of hot and humid environments on ECC material performance. To examine the effects of environmental exposure, hot water immersion was performed on individual fibers, single fibers embedded in an ECC matrix, and composite ECC material specimens [16]. Specimens for both individual fiber pullout and composite ECC materials were cured for 28 days at room temperature prior to immersion in hot water at 60ºC for up to 26

weeks.

After 26 weeks in hot water immersion, little change was seen in mechanical fiber properties such as fiber strength, fiber elastic modulus, and elongation. Interfacial properties, however, experienced significant changes, particularly between 13 and 26 weeks of hot water immersion. During this time, the chemical bonding between fiber and matrix strengthened significantly, while the apparent strength of the fiber dropped. These two phenomena caused fibers within the ECC matrix to delaminate and break during loading after 26 weeks of immersion, rather than pull-out intact, as seen in specimens immersed 13 weeks or less. This change in interfacial properties resulted in a drop of ultimate strain capacity, as predicted from the ECC micromechanical design model. The strain capacity of the ECC material dropped from 4.5% at early age to 2.75% after 26 weeks of hot water immersion.

Using Life Cycle Assessment to Guide Sustainable ECC Overlay Design

Life cycle assessment (LCA) is an analytical technique for assessing potential environmental burdens, social impacts, and economic costs thereby measuring progress toward sustainability [17]. Together these broad metrics form the triple bottom line of current sustainability indicators. Based on defined framework boundary, LCAs quantify the potential consumption and impacts throughout a product's life cycle from raw material acquisition through production, use, and disposal [18]. An LCA model of a pavement overlay system was developed by Zhang et al. [19] and its application to ECC overlays is presented.

Life Cycle Model

The LCA model for pavement overlays divided into six modules: material production, consisting of the acquisition and processing of raw materials; construction, including all construction processes, maintenance activities, and related construction machine usage; distribution, accounting for transport of materials and equipment to and from the construction site; traffic congestion, which models all construction and maintenance related traffic congestion; usage, including overlay roughness effects on vehicular travel and fuel consumption during normal traffic flow; and end of life, which models demolition of the overlay and processing of the materials. Details of each module are described in Zhang et al. [19]. Input and output data from each module are evaluated to capture the material consumption, energy consumption, and environmental impacts of the overlay system throughout its service life. Several datasets are required to provide the life cycle information for input materials or processes. For example, the dataset for ECC production provides the raw material consumption, total primary energy consumption, pollutant emissions, and wastes associated with producing a unit volume of ECC. Raw material consumption quantifies the non-fuel material inputs, such as the mass of cement required. Total primary energy consumption includes the energy required for extraction, refining, transportation, and processing the material. The air and water pollutant emissions and solid wastes are also modeled for each life cycle stage. These datasets and sources can be found in Keoleian and Kendall [20] and Zhang et al. [19].

The LCA model is linked to four external models: (1) a material environmental impact model, SimaPro 7.0 developed by Pre Consultants [21]; (2) a vehicle emissions model, MOBILE 6.2 developed by U.S. Environmental Protection Agency (EPA) [22], and four localized MOBILE 6.2 data inputs for the winter and summer seasons which include annual temperature range, Reid vapor pressure, age distribution of the vehicle fleet, and average vehicle miles traveled data [23]; (3) a construction equipment model, NONROAD, also developed by the EPA [24]; (4) and a traffic flow model developed at the University of Kentucky [25].

Green ECC Materials and Pavements

As described earlier by Lepech et al. [26], a total of 14 ECC mixes were designed incorporating a variety of industrial waste streams. These wastes include fly ash from coal-fired thermoelectric power generation, a variety of sands and wastes from metal casting processes, post consumer carpet fibers, wasted cement kiln dust from cement production, and expanded polystyrene (EPS) beads from lost foam foundry operations. The mix proportions and material properties of these mix designs are shown in Table 1. The incorporation of industrial wastes is governed by micromechanical models for the design of ECC materials as described in Lepech et al. [2, 27].

A set of metrics capturing consumption and environmental impacts was computed for each of the 14 mix designs. These values result from a life cycle inventory assembled for cement-based materials and summarized by Kendall et al. [18]. These values are shown in Table 2.

To assess the impact of green ECC mix designs on the larger rigid pavement overlay system, a series of structural design charts were developed by Qian [29] for concrete and ECC overlays. These structural design charts are based on finite element modeling (FEM) modeling of ECC and concrete overlaying a cracked concrete substrate. This is shown in Fig. 6. Using this model, a relationship between maximum stress developed during edge loading of a one equivalent single axle load (ESAL) ($80kN$) dual axle load and overlay thickness were determined. Existing slab and subgrade parameters were held constant ($E_{existing} = 20.7GPa$, $k_{subgrade} = 27.1MN/m^3$). The elastic modulus of the ECC overlay was also held constant at $20.7GPa$ for all mix designs. For the design of a concrete overlay, the elastic modulus was increased to $34.5GPa$.

From the FEM model, the following overlay design chart was developed, relating overlay design thickness with the maximum stress level in the overlay. This relationship is shown in Fig. 7. For validation of FEM results, maximum stresses in an uncracked substrate scenario were compared to the classical Westergaard solution for maximum tensile stress within a semi-infinite pavement slab under edge loading [30]. As the size of the slab within the FEM model increases, the maximum tensile stress within the system approaches the Westergaard solution asymptotically as expected.

Sustainability Metrics for ECC Pavement Overlays

As summarized by Zhang et al. [19] total life cycle results represent the environmental impacts the material module, construction module, distribution module, traffic congestion module, usage module, and

Table 1. Material Mix Proportions and Materials Properties (kg/m^3 Unless Noted Otherwise).

Mix	Cement	Sand	Gravel	Water	Foundry Sand	Fly Ash	CKD	EPS	Carpet Fiber	PVA Fiber	PE Fiber	HRWR	HPMC	MPR (MPa)	ε_μ (%)	f'_c (MPa)
1	579	462		319		693				26		7.51		13.4	3	55
2	414	456		319		829				26		5.8		12.4	4	46
3	324	453		317		907				26		5.18		10.8	4	38
4	1266	633		321							20	12.6	0.63	12.2	4	65
5	845	845		361						26		16.9	1.3	7.8	5	57
6	590	472		288		708				26		19.3		8.9	5	54
7	322	709		281		709				26		19.3	0.16	10	4	54
8	322	709		281		709				26		19.3	0.16	10.5	4	55
9	373	822		325		448				26		22.4	0.28	8.4	4	57
10	583			298	467	700				26		17.5		6.8	4	46
11	578			319	462	693				26		7.51		10.5	4	55
12	578	462		319		693			26	23		13		8.6	4	55
13	321			319	462	693	347			26		7.51		9.5	4	54
14	519	355		239		503		6		26		1.25		8.4	4	45
Concrete	390	376	1041	166										7.2	0	47

CKD - Cement Kiln Dust; EPS - Expanded Polystyrene; PVA - Polyvinylalcohol; PE - Polyethylene; HRWR - High Range Water Reducer; HPMC - Hydroxypropylmethyl Cellulose; MOR - Modulus of Rupture, ε_u - ultimate tensile strain capacity.

Table 2. Consumption and Environmental Impacts per m^3 for Individual Mix Designs [28].

Mix	Tot E (GJ)	CO_2 (kg)	NO_x (kg)	PM_{10} (mg)	SO_x (kg)	BOD (kg)
1	6.69	670	3.55	5.88	2.62	0.21
2	5.56	506	2.97	5.7	1.98	0.21
3	4.95	416	2.63	5.75	1.63	0.21
4	9.11	1,228	4.46	9.5	2.82	0.16
5	7.6	876	3.73	6.82	2.08	0.21
6	6.03	634	3.04	4.63	1.56	0.21
7	4.74	401	2.37	3.03	1.04	0.21
8	4.74	401	2.37	3.03	1.04	0.21
9	5.07	450	2.51	3.51	1.15	0.21
10	5.49	573	2.87	3.74	1.42	0.21
11	5.7	609	2.97	4.01	1.5	0.21
12	5.7	615	2.86	4.53	1.5	0.21
13	3.85	296	2.08	1.6	0.82	0.21
14	5.04	476	2.59	3.29	1.21	0.21
Concrete	2.46	373	1.06	3.47	0.81	0

Fig. 7. Design Chart for ECC and Concrete Overlay Thickness [29].

Fig. 6. FEM Model of Overlay System with Existing Cracked Concrete Substrate [29].

end of life module over a 40-year service life. The environmental indicators in this study include energy consumption and greenhouse gas emissions.

The primary energy consumptions for 10 kilometers of the concrete, ECC and hot mixed asphalt (HMA) overlay are 6.8×10^5, 5.8×10^5, and $2.1 \times 10^6 GJ$, respectively. As shown in Fig. 8, the life cycle energy consumption for the three systems is dominated by material production energy, traffic congestion related energy, and roadway roughness energy. Roughness related fuel consumption has not been previously studied using LCA methods. Without considering surface roughness effects, the life cycle energy consumptions of three overlay systems decreases by 23, 36, and 14%, respectively.

Due to the ductile behavior of ECC materials, the ECC overlay uses about 15 and 72% less energy than the concrete overlay and the HMA overlay, respectively (Fig. 8). The high energy consumption
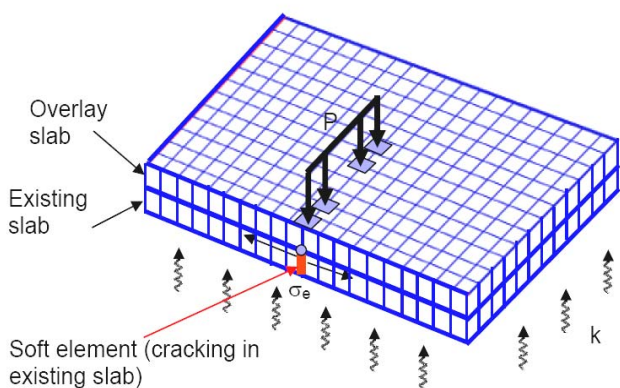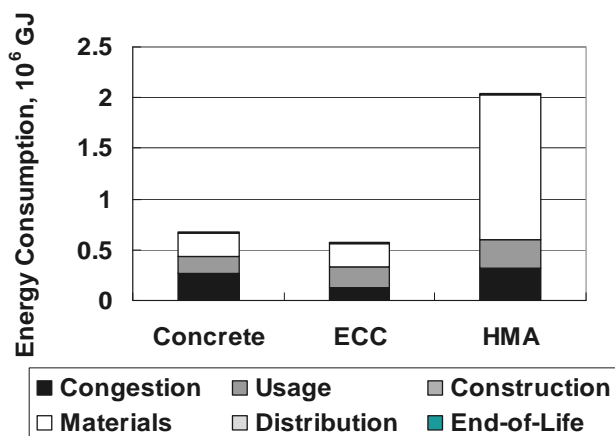
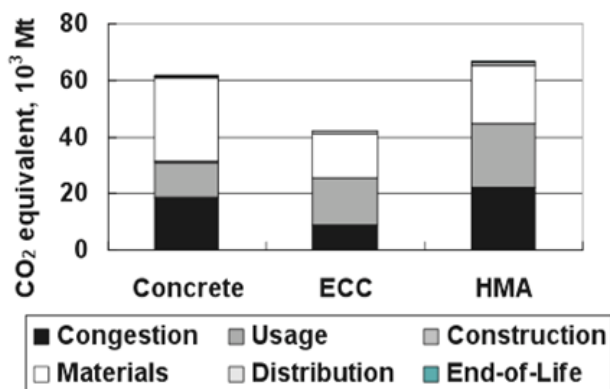Fig. 8. Primary Energy Consumption by Life Cycle Phase [19].

Fig. 9. Greenhouse Gas Emissions by Life Cycle Phase [19].

for an HMA overlay is caused by the high feedstock energy contained in asphalt which accounts for 30% of the total life cycle primary energy consumption for HMA system.

Greenhouse gas (GHG) emissions inventoried in this study include CO_2, methane, and nitrous oxide. The global warming impact is characterized by GHG emissions in metric tons of CO_2 equivalent. This is calculated by multiplying the mass of each GHG emission by its global warming potential (GWP), where GWP for CO_2 is 1, for methane is 23, and for nitrous oxide is 296 [31]. Fig. 9 shows the global warming impact of each overlay system.

CO_2 emissions significantly dominate the contribution to global warming impact. In the concrete overlay system CO_2 represents 99.2% of total life cycle GWP, in the ECC system CO_2 represents 99.4% of total life cycle GWP, and in the HMA system CO_2 represents 94.4% of total life cycle GWP. The ECC system reduces GHG emissions by 32 and 37% compared to the concrete overlay system and HMA overlay system, respectively. Generally, CO_2 emissions reflect energy consumption; however, cement production releases CO_2 during calcination of limestone. Additionally, a large amount of primary energy consumption in the HMA overlay system is the feedstock energy. Carbon embodied in the material is fixed and does not generate CO_2 unless it is burned. This relationship is evident in the comparison of Figs. 8 and 9 wherein the CO_2 emission of the HMA overlay system is not significantly higher than the other two systems.

ECC Bridge Demonstration Applications

Bridge Deck Patching

In 2004, a MDOT owned two-lane bridge overpassing a four-lane expressway was selected for a ECC pavement patching demonstration. This bridge, constructed in 1976, is a four span, simply supported, steel girder bridge with a nine inch thick reinforced concrete deck. Average daily traffic (ADT) for this structure was recently counted by the Washtenaw County Road Commission at 3,000 vehicles per day. However, while ADT is relatively low, a large number of 11-axle gravel trucks use this structure as a truck route, greatly increasing loads on the bridge. Required patch work consisted of roughly a 7×9*m* section of severely deteriorating asphalt patching, which had been used to temporarily repair a section of the concrete deck.

Long term performance of both the ECC patch and adjacent concrete patch was recorded through a series of site visits. During visits, pictures were taken to document crack development and crack patterns, cracking along the interface between existing deck and repair material, and the overall condition of both repairs. Initial visits conducted 2 days after patching showed no visible cracking in the ECC, while a clearly visible crack, approximately 300*mm* wide, had appeared in the concrete patch, most likely due to shrinkage deformation. After 4 months of winter exposure, a number of small microcracks, each roughly 50*mm* wide, had formed within the ECC patch, while the concrete crack observed shortly after casting had widened to 2*mm* and was surrounded by deteriorated and spalling concrete. Observations made 10 months after patching revealed a maximum ECC crack width of 50*mm*, while sections of the concrete patch were severely deteriorating. In total, the repaired bridge deck experienced more than five complete Michigan winter cycles of freezing and thawing, in addition to live loads before deck reconstruction was carried out. During these years the ECC patch repair survived the combined environmental/live loading environment with minor microcracking limited to less than 50*μm*. In contrast, the concrete repair portion developed localized cracks in excess of 3.5*mm* wide and required re-repair in 2005. The development of crack width over time in both ECC and concrete patches is shown in Fig. 10. From this comparison of adjacent patch sites subjected to identical loading, ECC demonstrated improved performance as compared to concrete immediately after casting, and improving over time.

Bridge Deck Link Slab

One of the main durability and maintenance problems confronting departments of transportation nationwide are the continual failure of mechanical expansion joints installed between adjacent simple span bridge decks. While these expansion joints are essential to accommodate the large thermal deformations of the nearby decks, their tendency to quickly fall into disrepair and eventually leak is a constant source of deterioration of the entire superstructure. Water from the deck, saturated with de-icing salts during cold weather, leaks through deteriorated joints and ultimately corrodes the ends of steel girders, or penetrates into precast concrete girders and corrodes the reinforcing steel.
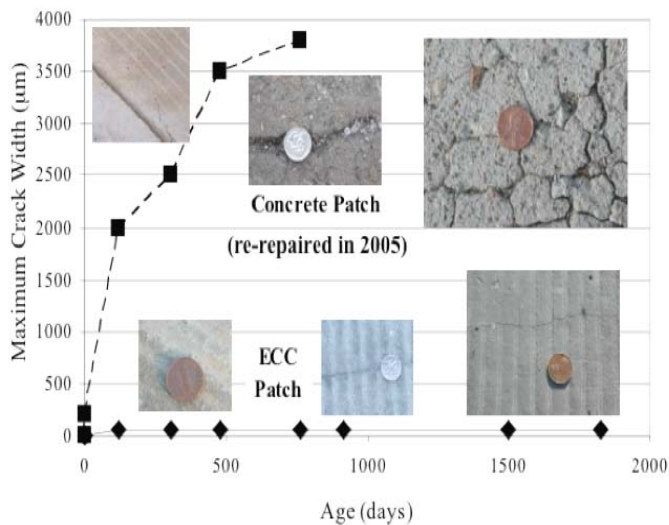
Fig. 10. Development of Crack Width over Time in ECC and Concrete Patch [15].
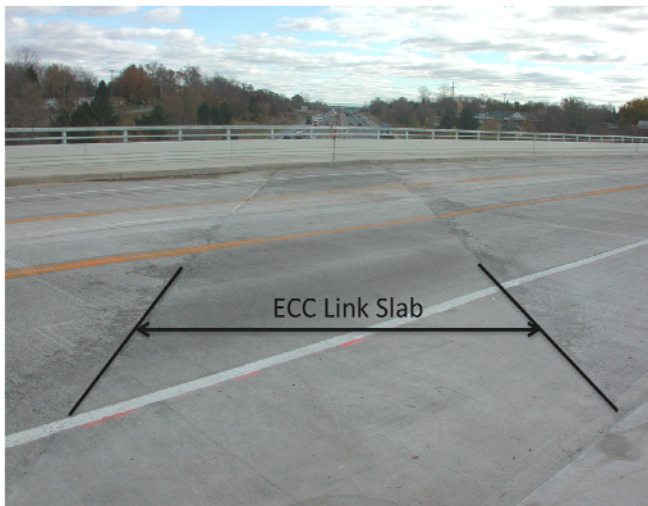

Fig. 11. Constructed ECC Link Slab.

To allow bridge designers to maintain simple span design assumptions, and allow for retrofitting of existing bridge structures, the use of ECC "link slabs", rather than mechanical expansion joints between adjacent bridge spans, has been demonstrated by the MDOT [32]. By removing the expansion joint and replacing a portion of the two adjacent decks with section of ECC material overtop the joint, a continuous deck surface is constructed. The unique capability of ECC material to deform up to 4% strain in uniaxial tension while maintaining low crack widths allows the ECC link slab to accommodate the deformations imposed by the adjacent decks (i.e. due to thermal expansion and contraction) while protecting the underlying superstructure and substructure from corrosives present on the deck surface.

Large scale laboratory testing of ECC link slabs was conducted to investigate the load capacity and fatigue performance of ECC link slabs, along with the development of cracking on the tensile face of the ECC link slab. For comparison purposes, a concrete "link slab" was also tested for load capacity, fatigue performance, and crack width development. This testing program is summarized by Kim et

al. [33]. This study found that ECC material was a suitable choice for construction of link slabs to replace conventional mechanical expansion joints. The large tensile strain capacity, facilitated by saturated multiple cracking with widths of 60*mm* meet all structural and durability needs of a link slab application. During monotonic loading, a lower stress in the reinforcement was seen in ECC link slabs than in concrete link slabs, allowing for further reduction of reinforcement levels. Cyclic tests revealed that both ECC and concrete link slabs show no degradation of stiffness after 100,000 loading cycles. However, crack widths in the concrete link slab grew to over 600*mm* during cyclic testing while crack widths in the ECC link slab remained small, in all cases less than 60*mm*. This allows ECC link slabs to better meet the durability and serviceability requirements and better protect underlying bridge superstructure and substructure.

As noted previously, the MDOT completed a demonstration ECC link slab project during Summer 2005. This ECC link slab measured 5.5×20.25*m*. Construction was comprised of 25.5*m³* of ECC, delivered on-site in standard ready-mix concrete trucks from a nearby batching plant. The constructed link slab is shown in Fig. 11.

Conclusion

Engineered Cementitious Composites (ECC) exhibit many of the characteristics desirable for high performance pavement applications, including excellent durability, high ductility, and resistance to cracking. As compared to plain concrete, ECC material tests show improved performance in shrinkage cracking behavior, fatigue and substrate bond testing, freeze thaw exposure, abrasion and wear testing, long term material performance, and accelerated weather tests. Furthermore, the use of ECC materials in demonstration projects with the Michigan Department of Transportation, including bridge deck patching and a link slab project, reveal that ECC is a viable high performance material choice for various transportation applications.

Using sustainability metrics, ECC materials have shown to be beneficial when designed to properly leverage the material characteristics of ECC. The use of greener cementitious materials for rehabilitation of rigid pavement systems represents a large potential for the reduction of material and energy resource consumption and pollutant emissions. Additionally, the incorporation of industrial waste streams into new overlay materials can successfully divert large waste flows from landfills. However, the incorporation of such industrial wastes must be carefully controlled to maintain overall system performance over the entire design life cycle.

As was found by the co-authors and others, a properly designed ECC overlay system had lower environmental burdens over a 40-year service life as compared to concrete and HMA overlay systems. By extending the service life and minimizing maintenance frequency, the ECC overlay system reduces total life cycle energy by 14%, GHG emissions by 32%, and costs by 40% as compared to conventional overlays. Material, traffic, and pavement roughness effects were identified as the life cycle stages with greatest environmental impacts throughout the overlay system life cycle. Alternative overlay design strategies, such as varying overlay thickness and different maintenance schedules, can be implemented

based on local traffic conditions and pavement requirements to achieve even further improvements. Using the presented approach of LCA-guided materials and pavement design, pavement engineers are better able to incorporate high performance pavement materials into applications through quantifiable sustainability indicators and long-proven pavement design methods.

Acknowledgements

References

1. Research and Innovative Technology Administration (RITA), (2008). *Transportation Statistics Annual Report - 2008*, US Department of Transportation, Washington, DC, USA.

2. Battelle Group, (2002). *Towards a Sustainable Cement Industry*, World Business Council for Sustainable Development, Geneva, Switzerland.

3. American Society of Civil Engineers, (2009). *Report Card for America's Infrastructure - 2009*, American Society of Civil Engineers, Restion, Virginia, USA.

4. Li, V.C., (1993). From Micromechanics to Structural Engineering - The Design of Cementitious Composites for Civil Engineering Application, *JSCE Journal of Structural Mechanics and Earthquake Engineering*, 10(2). pp. 37-48.

5. Weimann, M.B. and Li, V.C., (2003). Drying Shrinkage and Crack Width of ECC, *Seventh International Conference on Brittle Matrix Composites*, pp. 37-46, Warsaw, Poland.

6. Fischer, G. and Li, V.C., (2003). Deformation Behavior of Fiber-Reinforced Polymer Reinforced Engineered Cementitious Composite (ECC) Flexural Members under Reversed Cyclic Loading Conditions, *ACI Structural Journal*, 100(1), pp. 25-35.

7. Lepech, M.D. and Li, V.C., (2009). Water Permeability of Engineered Cementitious Composites, *Cement and Concrete Composites*, 31(10), pp. 744-753.

8. Yang, Y., Lepech, M.D., Yang, E.H., and Li, V.C., (2009). Autogenous Healing of Engineered Cementitious Composites Under Wet-Dry Cycles, *Journal of Cement and Concrete Research*, 39(5), pp. 382-390.

9. Lepech, M.D. and Li, V.C., (2008). Large Scale Processing of Engineered Cementitious Composites, *ACI Materials Journal*, 105(4) pp. 358-366.

10. Zhang J. and Li, V.C., (2002). Monotonic and Fatigue Performance in Bending of Fiber Reinforced Engineered Cementitious Composite in Overlay System, *Journal of Cement and Concrete Research*, 32(3), pp. 415-423.

11. Maalej, M., Hashida, T., and Li, V.C., (1995). Effect of Fiber Volume Fraction on the Off-Crack-Plane Fracture Energy in Strain-Hardening Engineered Cementitious Composites, *Journal of the American Ceramic Society*, 78(12), pp. 3369-3375.

12. Li, V.C., (2003). Durable Overlay Systems with Engineered Cementitious Composites (ECC), *International Journal for Restoration of Buildings and Monuments*, 9(2), pp. 215-234.

13. Sahmaran, M. and Li, V.C., (2007). De-icing Salt Scaling Resistance of Mechanically Loaded Engineered Cementitious Composites, *J. Cement and Concrete Research*, 37(7), pp. 1035-1046.

14. Michigan Department of Transportation, (2001). *Michigan Test Method 111 - Determining an Aggregate Wear Index (AWI) By Wear Track Polishing Tests*, Michigan Department of Transportation, Lansing, Michigan, USA.

15. Li, V.C. and Lepech, M.D., (2004). Crack Resistant Concrete Material for Transportation Construction, *Transportation Research Board 83rd Annual Meeting Compendium of Papers*, Paper No. 04-4680, Washington, DC, USA.

16. Li, V.C., Horikoshi, T., Ogawa, A., Torigoe, S., and Saito, T., (2004). Micromechanics-based Durability Study of Polyvinyl Alcohol-Engineered Cementitious Composite (PVA-ECC), *ACI Materials Journal*, 101(3), pp. 242-248.

17. Keoleian, G.A. and Spitzley, D.V., (2006). *Sustainability Science and Engineering*, Elsevier, the Netherlands.

18. The International Organization for Standardization (ISO), (1997). *Environmental Management: Life Cycle Assessment: Principles and Framework*, ISO, Geneva, Switzerland.

19. Zhang, H., Lepech, M.D., Keoleian, G., Qian, S., and Li, V.C., (2009). Dynamic Life Cycle Modeling of Pavement Overlay Systems: Capturing the Impacts of Users, Construction, and Roadway Deterioration, *Journal of Infrastructure Systems*, http://dx.doi.org/10.1061/(ASCE)IS.1943-555X.0000017, (Article in Press)

20. Keoleian, G.A. and Kendall, A., (2005). Life Cycle Modeling of Concrete Bridge Design: Comparison of Engineered Cementitious Composite Link Slabs and Conventional Steel Expansion Joints, *Journal of Infrastructure Systems*, 11(1), pp. 51-60.

21. Product Ecology Consultant (Pre), (2004). *SimaPro 6.0.*, Pre: Utricht, the Netherlands.

22. United States Environmental Protection Agency (EPA), (2002). *MOBILE 6.2*, United States Environmental Protection Agency, Ann Arbor, Michigan, USA.

23. Southeast Michigan Council of Governments (SEMCOG), (2006). *Ozone and Carbon Monoxide Conformity Analysis for the Proposed Amendment of the 2030 Regional Transportation Plan for Southeast Michigan*, Southeast Michigan Council of Governments, Detroit, Michigan, USA.

24. United States Environmental Protection Agency (EPA), (2005). *NONROAD2005 Model*, United States Environmental Protection Agency, Ann Arbor, Michigan, USA.

25. Kentucky Transportation Center (KTC), (2002). The Costs of Construction Delays and Traffic Control for Life-cycle Cost

Analysis of Pavements, *Report No. KTC-02-07/SPR197-99 and SPR218-00-1F*, University of Kentucky, Lexington, Kentucky, USA.

26. Lepech, M.D., Keoleian, G.A., Qian, S., and Li, V.C., (2008). Design of Green Engineered Cementitious Composites for Pavement Overlay Applications, *First International Symposium on Life-Cycle Civil Engineering,* pp. 907-912, Varenna, Lake Como, Italy.

27. Lepech, M.D., Li, V.C., Robertson, R.E., and Keoleian, G.A., (2008). Design of Green Engineered Cementitious Composites for Improved Sustainability, *ACI Materials Journal* 105(6), pp. 567-575.

28. Kendall, A., Keoleian, G., and Lepech, M.D., (2008). Materials Design for Sustainability through Life Cycle Modeling of Engineered Cementitious Composites, *Materials and Structures*, 41(6), pp. 1117-1131.

29. Qian, S., (2007). Incfluence of Concrete Material Ductility on the Behavior of High Stress Concentration Zones, *PhD Dissertation,* University of Michigan, Ann Arbor, Michigan, USA.

30. Westergaard, H., (1926). Stresses in Concrete Pavements Computed by Theoretical Analysis, *Public Roads*, 7(2), pp. 25-35.

31. Intergovernmental Panel on Climate Change (IPCC), (2007). *Fourth Assessment Report - AR4*, Cambridge University Press, Cambridge, United Kingdom and New York, NY, USA.

32. Lepech, M.D. and Li, V.C., (2009). Application of ECC for Bridge Deck Link Slabs, *Materials and Structures*, 42(9), pp. 1185-1195.

33. Kim, Y.Y., Fischer, G., and Li, V.C., (2004). Performance of Bridge Deck Link Slabs Designed with Ductile ECC, *ACI Structural Journal*, 101(6), pp. 792-801.